Organic & Biomolecular Chemistry

COMMUNICATION

Dual Emissive Bodipy-Benzodithiophene-Bodipy TICT Triad with Remarkable Stokes Shift of 194 nm

Sanchita Sengupta[a,b*], Upendra K. Pandey[a]

An acceptor-donor-acceptor (A-D-A) triad based on BODIPY acceptor and benzodithiophene donor exhibited dual fluorescence and pronouned fluorescence solvatochromism because of twisted intramolecular charge transfer (TICT) state formation. Furthermore, it showed a Stokes shift of ~ 194 nm which is highest known for any BODIPY compound with readily tunable fluorescence and high charge carrier mobility of 4.46 × 10⁻⁴ cm²/Vs.

Molecular design of twisted donor-acceptor (D-A) systems largely govern their photophysical properties in solution[1–4] such as excimer formation,[2] twisted intramolecular charge transfer (TICT) states[5,6] and aggregate induced emission (AIE).[7–11] Excimer emission in BODIPY[12] based D-A molecules and their dimeric systems have been vastly explored.[2,13] Depending upon geometry and twisting of the D-A backbone and their decoupling by spacer units, they show intense solvatochromism[14,15] as well as exciplex formation,[16,17] mechanofluorochromism,[18,19] AIE[7] or TICT states.[20] Hence, judicious molecular engineering of D-A system with spacer unit that decouples the donor and acceptor should lead to new fluorescence probes with interesting photophysical phenomena such as TICT and AIE. TICT property can be exploited for designing new materials with potential applications in chemosensors, in lighting and display such as organic light emitting diodes (OLEDs)[21–23], non linear optics[24] and optical waveguides. Moreover, such systems could have potential applications in biomedical imaging[25], optoelectronic devices such as in organic photovoltaics (OPV).[26]

Benzodithiophene (BDT) is an interesting candidate for OPV applications owing to their planar structure, deep lying HOMO levels and reportedly high hole mobilities as well as high power conversion efficiencies (PCEs) in organic and polymer solar cells.[27–29] Recently, we reported regioisomeric D-A triads based on BDT donors and BODIPY acceptor, **T1** and **T2** (Figure 1) that showed efficient photoinduced electron transfer (PET) and possess appreciable charge carrier mobilities.[30] D-A systems composed of BDT and BODIPY usually absorb in the ultraviolet (UV) and the visible region with spectral coverage of upto ~ 700 nm as a result of intramolecular charge transfer.[13] Density functional theory (DFT) calculations revealed that the optical and redox properties can be extensively tuned either by changing substituents or by tuning the coupling position of BDT donor at either meso position or at α/β positions of BODIPY. But reports of BODIPY based TICT and AIE systems are rather scarce.[31,32]

Herein, we report the design, synthesis and photophysical properties of a new acceptor-donor-acceptor triad system **A-D-A** (Figure 1) based on BODIPY acceptor and BDT donor whereby the BODIPY units are attached through their meso positions and are decoupled from the donor units by two flexible phenyl spacers. We intend to study the optical properties of **A-D-A** compared to the previously studied D-A-D compounds that showed efficient PET.[30] The photophysical properties of **A-D-A** triad were investigated using steady state absorption, fluorescence spectroscopy, fluorescence lifetimes and solvatochromism. Moreover, charge carrier mobility of this material was investigated in order to assess its suitability for optoelectronic applications.

[a]*Interdisciplinary Centre for Energy Research (ICER)*
Indian Institute of Science (IISc) Bangalore
C. V. Raman Road, Bangalore 560012, Karnataka, India.
Present Address: [b]*Department of Chemical Sciences, Indian Institute of Science Education and Research (IISER) Mohali*
Sector 81, Knowledge City, P.O. Manauli 140306, Punjab, India.
E-mail: sanchita@iisermohali.ac.in
Electronic Supplementary Information (ESI) available: Synthesis details, compound characterization and spectroscopic characterization.
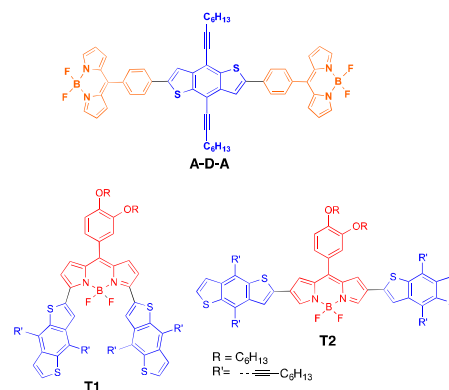See DOI: 10.1039/x0xx00000x

Fig 1. Molecular triad(s) newly synthesized (**A-D-A**) and investigated (**T-1**, **T-2** and **A-D-A**) in this work.

Organic & Biomolecular Chemistry

COMMUNICATION

The synthesis of **A-D-A** was carried out as outlined in Scheme 1. BODIPY **4** was synthesized starting from 4-bromobenzaldehyde and pyrrole in presence of catalytic amount of HCl in an aqueous media according to a reported procedure[34,35] for a different dipyrromethane (DPM) compound. However, it is to be noted here that this reaction in an aqueous medium has not been used for the synthesis of DPM **3** and BODIPY **4** earlier to the best of our knowledge. This method[34] was advantageous in terms of yield (78 %) compared to the conventional route of condensation of pyrrole with aldehyde in presence of catalytic amount of trifluoroacetic acid (TFA). Distannylated BDT (**5**) was synthesized according to previously reported procedure (see ESI).[33] Synthesis of **A-D-A** was achieved by Stille coupling of **4**[22] (2 eq.) and **5** in dry toluene with catalytic amounts of tris(dibenzylidene-acetone)dipalladium(0), $Pd_2(dba)_3$ and tri(o-tolyl)phosphine $P(o\text{-tol})_3$[28] and **A-D-A** was isolated in 56 % yield (ESI for details).

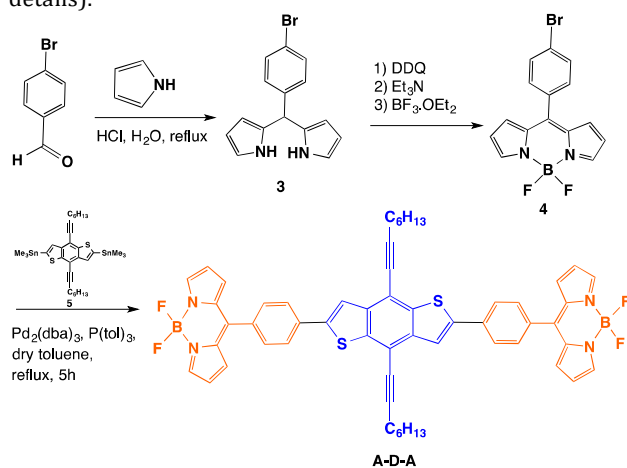**Scheme 1.** Synthesis of BDT-BODIPY triad **A-D-A**.

Fig. 2 shows the UV/Vis absorption spectra of model acceptor and donor compounds **4** and **5** and triad **A-D-A** in DCM. Donor **5** has absorption maximum at 372 nm while the absorption maximum for acceptor **4** occurs at 504 nm. The absorption spectrum of **A-D-A** is merely the sum of D and A absorption i.e., absorption maxima at 315 nm, 380 nm for the BDT donor and at 503 nm for the BODIPY unit, indicative of no electronic communication between the donor and acceptor components.
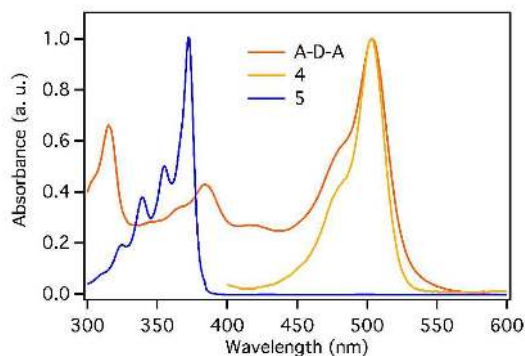

Fig 2. UV-Vis absorption spectra of model compounds **5**, **4** and triad **A-D-A** in DCM.

The highest occupied molecular orbital (HOMO) and lowest unoccupied molecular orbital (LUMO) levels of **A-D-A** were calculated by density functional theory (DFT) method using Gaussian 09 package by B3LYP/6-31G(d,p) method.[36] For **A-D-A**, HOMO is entirely localized on the BDT unit and the LUMO is entirely localized on BODIPY with no overlap between the HOMO and LUMO (Fig. 3). Hence, no electronic communication was observed between BDT and BODIPY that is in agreement with the experimental absorption spectrum of **A-D-A**. The corresponding frontier molecular orbital (FMO) energies are presented in Table S1. Geometry optimization was carried out on **A-D-A** structure and torsion angles between BODIPY and phenyl spacer and between phenyl spacer and BDT unit were 54.1° and 32.2° respectively, which render the molecule non-planar. Furthermore, charge distribution calculations were performed including dipole moments for the ground state and the excited state of **A-D-A**. Notably, the ground state
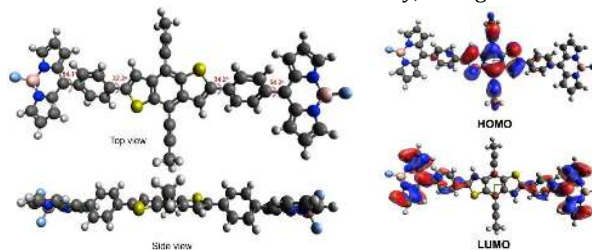
dipole moment of 1.28 D was obtained for **A-D-A** whereas dipole moment of the first excited state obtained was much higher ~ 1.94 D. This difference in dipole moments in ground and excited state has important consequences in the optical properties of **A-D-A** as will be discussed (vide infra).

Fig 3. Optimized structure of **A-D-A** showing dihedral angles in top view and side view showing phenyl groups twisted out of the plane of the structure.

Cyclic voltammetry (CV) measurements were performed to determine the frontier orbital energy levels of **A-D-A**. Based on the first oxidation potential onset (E_{ox}^{onset}) and first reduction potential (E_{red}^{onset}), the HOMO was calculated as, HOMO = − (E_{ox}^{onset} + 4.76) eV[37] and LUMO = − (E_{red}^{onset} + 4.76) eV as summarized in Table S1. Accordingly, calculated HOMO and LUMO levels at ~ -5.86 eV and ~ -3.89 eV were obtained respectively for **A-D-A**. Fluorescence emission spectra of **A-D-A** (Fig. 4a) was measured upon three different excitations at 315 nm, 380 nm (donor) and 503 nm (acceptor) respectively. Notably, upon excitation at 315 nm and 380 nm, apart from the donor emission at 405 nm, a broad but intense emission was observed at ~ 698 nm which is attributed to a twisted intramolecular charge transfer state (TICT) state. Interestingly, a pseudo Stokes shift of ~ 194 nm (51546 cm⁻¹) was obtained which is remarkable and much higher than previous reports of high Stokes shifts for BODIPY compounds.[38–40] Fluorescence quantum yield was determined by absolute method using an integrating sphere set-up upon excitation at 383 nm and a quantum yield of ~ 0.03 was obtained for **A-D-A** (Table S2 in supporting information). The formation of TICT state is further justified by the high twist angles (BDP-phenyl and phenyl-BDT) in the structure as well as the difference in the DFT calculated dipole moments of ground state and first excited state. These dissimilar dipole moments lead to the preferential stabilization

Organic & Biomolecular Chemistry

of the excited state dipole over the ground state dipole of **A-D-A** in polar solvents. Therefore, the fluorescence shows bathochromic shift in solvents of increasing polarity.[14] Solvent dependent emission spectra were recorded for **A-D-A** (Fig. 4b) that showed significant bathochromic shift of the emission maximum from 549 nm in toluene to 647 nm in chloroform (CF) and 700 nm in DCM.
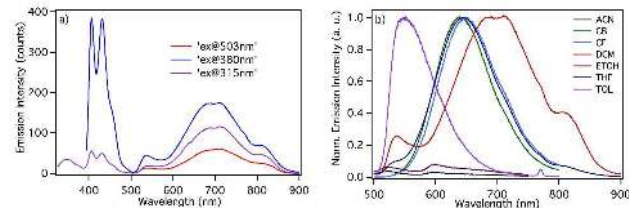

Fig 4. a) Fluorescence emission spectra of **A-D-A** in DCM; b) Fluorescence emission spectra of **A-D-A** upon excitation at 380 nm in acetonitrile (ACN), chlorobenzene (CB), chloroform (CF), ethanol (EtOH), toluene (Tol) and DCM.

Such pronounced positive solvatochromism is attributed to increased stabilization of a polar TICT state in polar solvents compared to a less polar ground state. Notably, UV-Vis absorption of **A-D-A** in the same solvents did not show any noticeable change, which is consistent with the fact that the ground state of **A-D-A** is less polar than the excited state. Fluorescence lifetime measurements were performed for donor **5** and **A-D-A** in CF using time correlated single photon counting (TCSPC) measurement technique. The fluorescence lifetimes of donor **D** was measured upon excitation at 374 nm and the decay was fast with a short lifetime of $\sim$ 0.47 ns. Fluorescence lifetime of **A-D-A** was measured upon excitation wavelength of 374 nm and decay profiles at emission wavelengths of 410 nm (corresponding to donor decay) and TICT emission at 700 nm were studied. The CT emission decay is known to exhibit longer rise time that is characteristic of charge transfer and a slow component, which is characteristic of the lifetime of the equilibrated molecules.[13] Accordingly, a slower decay was observed for **A-D-A** emission at 700 nm with a fluorescence lifetime of $\sim$3.41 ns as shown in Fig. 5a. Notably, the decay for the donor emission band of **A-D-A** at 410 nm was also fast with a lifetime of $\sim$ 0.79 ns which corresponds closely to that of the neat donor **5**. Fluorescence lifetime of **A-D-A** was also evaluated upon excitation at 469 nm and the lifetime of the TICT band at 700 nm was similar $\sim$ 3.40 ns (Table S3 for fluorescence decays, fitted parameters and lifetime values).
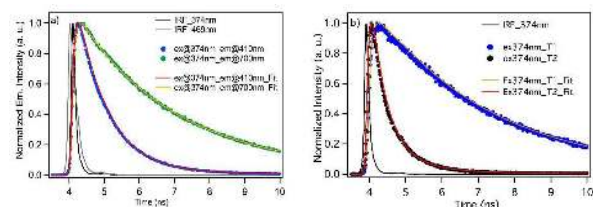

Fig 5. Fluorescence decay plots along with fitted data of a) triad **A-D-A** upon excitation at 374 nm and 469 nm; b) **T1** and **T2** upon excitation at 374 nm and 669 nm.

In order to understand the difference in the photophysics of **A-D-A** and previously reported regioisomers **T1** and **T2**, fluorescence lifetime measurements for **T1** and **T2** were performed. Lifetime measurements were carried out in CF upon excitation at 374 nm and 669 nm and the decay of

emission bands at 726 nm and 729 nm were studied for **T1** and **T2** respectively. The decay lifetime for the CT band of **T2** was $\sim$ 0.46 ns corresponding to a much faster decay compared to that of **T1** for which a longer lifetime of $\sim$ 3.16 ns was obtained (see supplementary information for fluorescence decays, fitted parameters and lifetime values). The faster decay and the shorter lifetime values for **T2** reflect that PET is more efficient in it than that for **T1**. Furthermore, it is noteworthy that the lifetime of **T1** ($\sim$ 3.16 ns) was marginally shorter than the lifetime of **A-D-A** ($\sim$ 3.41 ns) which corroborates the fact that TICT state formation in **A-D-A** is a slower process compared to PET that is occurring in **T1**.[41]

The formation of TICT state takes place in polar solvents and the TICT state reverses to the local excited (LE) state as the solvent polarity is reduced.[13] Emission measurements were performed in solvents of gradually decreasing polarity starting from 100 % THF upto 99/1 (v/v) hexane/THF. The formation of TICT in **A-D-A** was justified by the fluorescence spectrum showing an emission maximum at 650 nm. Upon reduction of the solvent polarity by gradual addition of hexane, the emission maximum shifted hypsochromically indicative of the formation of a LE state. Fig 6a shows the shift of emission maximum of **A-D-A** from 650 nm in 100 % THF to 523 nm in 99/1 (v/v) hexane/THF.

Triads **T1** and **T2** both showed ICT bands and electron transfer was more efficient in case of **T2** owing to its planar conformation. Interestingly, emission spectra of **T1** in hexane/THF solvent mixtures showed a negligible hypsochromic shift in fluorescence upon going from 100 % THF to increasing percentage of hexane in the hexane/THF mixtures. A negligible shift of $\sim$ 4-5 nm was observed which is attributed to the fact that the D and A units directly connected in **T1** without a phenyl spacer led to restricted rotation of the units leading to no significant solvatochromism (see supplementary information). In the case of **T2**, fluorescence was severely quenched as a result of efficient electron transfer.

Aggregate induced emission (AIE) is a highly desirable property for D-A compounds separated by spacer unit(s) for their potential application in OLEDs.[7,8] AIE property was investigated in **A-D-A** by measuring fluorescence in solvent mixtures of water and THF. Upon increasing fraction percentage of water (f_w) (from 0% to 10% to 30% upto 50 %), overall increased solvent polarity twisted the molecule and therefore shifted the equilibrium towards TICT state leading to a bathochromic shift from 645 nm to 657 nm. However, it is worth noting that the fluorescence intensity is severely quenched at 30% f_w and 50% f_w mixtures (Figure 6b). Upon increasing the f_w to 75% and 90 %, **A-D-A** preferably forms nanoclusters leading to restricted intramolecular rotation that renders the equilibrium shift towards LE state. Thus, in these two solvent mixtures (75% f_w and 90% f_w), hypsochromic shift of emission maximum at 633 nm was observed along with an increased fluorescence intensity (Figure 6b) because restricted motion lowered the pathways for non-radiative decay.
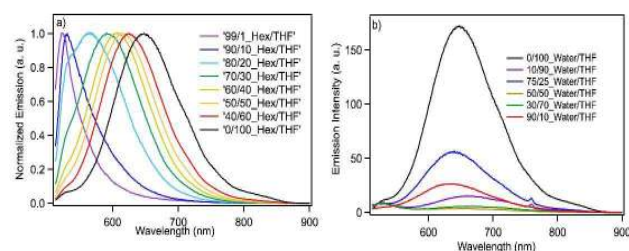
Organic & Biomolecular Chemistry

COMMUNICATION

Fig 6. a) Emission spectra of **A-D-A** in THF and THF/hexane mixtures with increasing volume percentages of hexane showing the formation of TICT state; b) AIE formation in **A-D-A** in various weight fractions of water and THF.

In order to assess the inherent charge transport properties of **A-D-A**, its hole mobility was measured using space charge limited current (SCLC) method.[42,43] Hole only device architecture of ITO/PEDOT:PSS/active layer (**A-D-A**)/Au was used to perform J-V characteristics in dark (see ESI†). Hole mobility of **A-D-A** was extracted from the SCLC region of the curve as shown in Fig. 7. Hole mobility of 4.46×10^{-4} cm^2/Vs was obtained for **A-D-A**. Higher mobility of **A-D-A** compared to the triads reported earlier (7.01×10^{-5} cm^2/Vs and 3.63×10^{-4} cm^2/Vs for **T1** and **T2** respectively)[30] can be attributed to the structure of **A-D-A** where electronically inactive alkyl chains are much less compared to those in the triads **T1** and **T2**[30] and consequently leads to better packing in films.
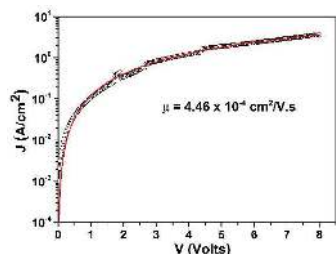

Fig 7. Dark J-V curve for triad **A-D-A** with a film thickness of 110 nm; the solid red line is the SCLC fit of the experimental data.

In summary, a new acceptor-donor-acceptor triad **A-D-A** based on BODIPY acceptor and BDT donor separated by phenyl spacers was synthesized that showed no ground state interaction between BODIPY and BDT units and spectral coverage till 550 nm. Interestingly, **A-D-A** showed dual emission with emission maximum at 700 nm that resulted due to the formation of a TICT state with a pseudo-Stokes shift of ∼ 194 nm. Furthermore, pronounced positive fluorescence solvatochromism was observed in solvents of increasing polarities due to the formation of TICT state. The formation of TICT state was further evident from emission measurements in solvent mixture of THF and hexane where a hypsochromic shift in emission of ∼ 127 nm was observed upon going from 100 % THF upto 99/1 (v/v) hexane/THF. Aggregate induced emission was observed for **A-D-A** in solvent mixtures of hexane/water with emission intensity and wavelength varying with increasing percentage of water indicating it suitability for possible OLED applications. Finally, high hole mobility of **A-D-A** of 4.45×10^{-4} cm^2/Vs was obtained that justified the suitability of this triad for (opto)electronic

applications such as in OLEDs and in OPV. At present, similar TICT based new molecules are being designed and their utility in (opto)electronic applications are being explored.

Notes and references

1. S. Sasaki, G. P. C. Drummen and G. Konishi, *J. Mater. Chem. C*, 2016, **4**, 2731–2743.
2. M. A. H. Alamiry, A. C. Benniston, G. Copley, A. Harriman and D. Howgego, *J. Phys. Chem. A*, 2011, **115**, 12111–12119.
3. J. Verhoeven, *Photochem. Photobiol. Sci.*, 2010, **9**, 1009–1017.
4. Z. R. Grabowski, K. Rotkiewicz and W. Rettig, *Chem. Rev.*, 2003, **103**, 3899–4032.
5. S. Sasaki, Y. Niko, A. S. Klymchenko and G. I. Konishi, *Tetrahedron*, 2014, **70**, 7551–7559.
6. H. Tanaka, K. Shizu, H. Nakanotani and C. Adachi, *Chem. Mater.*, 2013, **25**, 3766–3771.
7. Y. Hong, J. W. Y. Lam and B. Z. Tang, *Chem. Soc. Rev.*, 2011, **40**, 5361–5388.
8. J. Mei, Y. Hong, J. W. Y. Lam, A. Qin, Y. Tang and B. Z. Tang, *Adv. Mater.*, 2014, **26**, 5429–5479.
9. J. Shi, N. Chang, C. Li, J. Mei, C. Deng, X. Luo, Z. Liu, Z. Bo, Y. Q. Dong and B. Z. Tang, *Chem. Commun.*, 2012, **48**, 10675-10677.
10. H. Tsujimoto, D.-G. Ha, G. Markopoulos, H. S. Chae, M. A. Baldo and T. M. Swager, *J. Am. Chem. Soc.*, 2017, **139**, 4894-4900.
11. Y. Hong, J. W. Y. Lam and B. Z. Tang, *Chem. Commun.*, 2009, 4332-4353.
12. A. Loudet and K. Burgess, *Chem. Rev.*, 2007, **107**, 4891–4932.
13. R. Hu, E. Lager, A. Aguilar-Aguilar, J. Liu, J. W. Y. Lam, H. H. Y. Sung, I. D. Williams, Y. Zhong, K. S. Wong, E. Peña-Cabrera and B. Z. Tang, *J. Phys. Chem. C*, 2009, **113**, 15845–15853.
14. C. Reichardt, *Chem. Rev.*, 1994, **94**, 2319–2358.
15. A. Filarowski, M. Lopatkova, P. Lipkowski, M. Van der Auweraer, V. Leen and W. Dehaen, *J. Phys. Chem. B*, 2015, **119**, 2576–2584.
16. A. C. Benniston, G. Copley, H. Lemmetyinen and N. V Tkachenko, *ChemPhysChem*, 2010, **11**, 1685–1692.
17. X. K. Liu, Z. Chen, C. J. Zheng, C. L. Liu, C. S. Lee, F. Li, X. M. Ou and X. H. Zhang, *Adv. Mater.*, 2015, **27**, 2378–2383.
18. Z. Chi, X. Zhang, B. Xu, X. Zhou, C. Ma, Y. Zhang, S. Liu and J. Xu, *Chem. Soc. Rev.*, 2012, **41**, 3878–3896.
19. Y. Gong, Y. Zhang, W. Z. Yuan, J. Z. Sun and Y. Zhang, *J. Phys. Chem. C*, 2014, **118**, 10998–11005.

Organic & Biomolecular Chemistry

COMMUNICATION

20   J. T. Hynes, *Rev. Port. Quim.*, 1995, **2**, 12–17.

21   Q. Zhang, B. Li, S. Huang, H. Nomura, H. Tanaka and C. Adachi, *Nat. Photonics*, 2014, **8**, 326–332.

22   H. Kaji, H. Suzuki, T. Fukushima, K. Shizu, K. Suzuki, S. Kubo, T. Komino, H. Oiwa, F. Suzuki, A. Wakamiya, Y. Murata and C. Adachi, *Nat. Commun.*, 2015, **6**, 8476 (1-8).

23   S. Hirata, Y. Sakai, K. Masui, H. Tanaka, S. Y. Lee, H. Nomura, N. Nakamura, M. Yasumatsu, H. Nakanotani, Q. Zhang, K. Shizu, H. Miyazaki and C. Adachi, *Nat. Mater.*, 2014, **14**, 330–336.

24   N. B. Teran, G. S. He, A. Baev, Y. Shi, M. T. Swihart, P. N. Prasad, T. J. Marks and J. R. Reynolds, *J. Am. Chem. Soc.*, 2016, **138**, 6975–6984.

25   W. Zhang, Y.-Y. Ren, L.-N. Zhang, X. Fan, H. Fan, Y. Wu, Y. Zhang and G.-C. Kuang, *RSC Adv.*, 2016, **6**, 101937–101940.

26   M.-E. Ragoussi and T. Torres, *Chem. Commun.*, 2015, **51**, 3957–3972.

27   J. Hou, M.-H. Park, S. Zhang, Y. Yao, L.-M. Chen, J.-H. Li and Y. Yang, *Macromolecules*, 2008, **41**, 6012–6018.

28   T. Qin, W. Zajaczkowski, W. Pisula, M. Baumgarten, M. Chen, M. Gao, G. Wilson, C. D. Easton, K. Müllen and S. E. Watkins, *J. Am. Chem. Soc.*, 2014, **136**, 6049–6055.

29   Y. Huang, X. Guo, F. Liu, L. Huo, Y. Chen, T. P. Russell, C. C. Han, Y. Li and J. Hou, *Adv. Mater.*, 2012, **24**, 3383–3389.

30   S. Sengupta, U. K. Pandey and E. U. Athresh, *RSC Adv.*, 2016, **6**, 73645–73649.

31   W. G. Santos, J. Pina, H. D. Burrows, M. Forbes and D. R. Cardoso, *Photochem. Photobiol. Sci.*, 2016, **15**, 1124–1137.

32   D. Collado, J. Casado, S. R. González, J. T. L. Navarrete, R. Suau, E. Perez-Inestrosa, T. M. Pappenfus and M. M. M. Raposo, *Chem. Eur. J.*, 2011, **17**, 498–507.

33   Y. Liang, D. Feng, Y. Wu, S.-T. Tsai, G. Li, C. Ray and L. Yu, *J. Am. Chem. Soc.*, 2009, **131**, 7792–7799.

34   A. J. F. N. Sobral, N. G. C. L. Rebanda, M. da Silva, S. H. Lampreia, M. Ramos Silva, A. M. Beja, J. . Paixão and A. M. D. A. Rocha Gonsalves, *Tetrahedron Lett.*, 2003, **44**, 3971–3973.

35   A. K. Rawat and S. M. S. Chauhan, *Der Pharma Chem.*, 2014, **6**, 316–322.

36   R. C. 0. Gaussian 09, G. E. S. M. J. Frisch, G. W. Trucks, H. B. Schlegel, B. M. M. A. Robb, J. R. Cheeseman, G. Scalmani, V. Barone, H. P. H. G. A. Petersson, H. Nakatsuji, M. Caricato, X. Li, M. H. A. F. Izmaylov, J. Bloino, G. Zheng, J. L. Sonnenberg, T. N. M. Ehara, K. Toyota, R. Fukuda, J. Hasegawa, M. Ishida, J. Y. Honda, O. Kitao, H. Nakai, T. Vreven, J. A. Montgomery, E. B. J. E. Peralta, F. Ogliaro, M. Bearpark, J. J. Heyd, J. N. K. N. Kudin, V. N. Staroverov, T. Keith, R. Kobayashi, J. T. K. Raghavachari, A. Rendell, J. C. Burant, S. S. Iyengar, J. B. C. M. Cossi, N. Rega, J. M. Millam, M. Klene, J. E. Knox, R. E. S. V. Bakken, C. Adamo, J. Jaramillo, R. Gomperts, J. W. O. O. Yazyev, A. J. Austin, R. Cammi, C. Pomelli, G. A. V. R. L. Martin, K. Morokuma, V. G. Zakrzewski, A. D. D. P. Salvador, J. J. Dannenberg, S. Dapprich, J. C. O. Farkas, J. B. Foresman, J. V. Ortiz and 2010. and D. J. Fox, Gaussian, Inc., Wallingford CT, 2010.

37   G. Chen, H. Sasabe, Y. Sasaki, H. Katagiri, X.-F. Wang, T. Sano, Z. Hong, Y. Yang and J. Kido, *Chem. Mater.*, 2014, **26**, 1356–1364.

38   V. F. T. A. Y. Bochkov, I. O. Akchurin, O. A. Dyachenko, *Chem. Commun.*, 2013, 11653–11655.

39   A. Martin, C. Long, R. J. Forster and T. E. Keyes, *Chem. Commun.*, 2012, **48**, 5617-5619.

40   M. Bröring, R. Krüger, S. Link, C. Kleeberg, S. Köhler, X. Xie, B. Ventura and L. Flamigni, *Chem. Eur. J.*, 2008, **14**, 2976–2983.

41   R. Ghosh and D. K. Palit, *J. Phys. Chem. A*, 2015, **119**, 11128–11137.

42   J. C. Blakesley, F. A. Castro, W. Kylberg, G. F. A. Dibb, C. Arantes, R. Valaski, M. Cremona, J. S. Kim and J. S. Kim, *Org. Electron.*, 2014, **15**, 1263–1272.

43   J. Zhou, X. Wan, Y. Liu, Y. Zuo, Z. Li, G. He, G. Long, W. Ni, C. Li, X. Su and Y. Chen, *J. Am. Chem. Soc.*, 2012, **134**, 16345–16351.